Composites Part B 275 (2024) 111291

Contents lists available at ScienceDirect

Composites Part B

journal homepage: www.elsevier.com/locate/compositesb

Recycling of CF-ABS machining waste for large format additive manufacturing

Roo Walker [a,b], Matthew Korey [b,*], Amber M. Hubbard [b], Caitlyn M. Clarkson [b], Tyler Corum [a], Tyler Smith [a,b], Christopher J. Hershey [b], John Lindahl [b], Soydan Ozcan [b], Chad Duty [a,b]

[a] University of Tennessee – Knoxville, Knoxville, TN, USA
[b] Oak Ridge National Laboratory, Manufacturing Demonstration Facility, Oak Ridge, TN, USA

ARTICLE INFO

Handling Editor: Dr Uday Vaidya

ABSTRACT

Large format additive manufacturing (LFAM) necessitates the use of short fiber thermoplastic composites, such as carbon fiber filled acrylonitrile butadiene styrene, to enable printing. Currently, when LFAM parts are machined into their final shape, the machining scrap (*i.e.*, small flake like particles and offcuts) is landfilled. Previous studies have demonstrated the viability of recycling end-of-life LFAM parts by shredding and optionally re-compounding the material back into pellets. However, there is little understanding of the value and performance of recycled material made from LFAM machining scrap, which if pursued could motivate more broad recycling of this waste stream. In this study, recycled in-process machining scrap is explored as an LFAM feedstock source. Herein, it is found that the primary degradation mechanism of the recycled material is significant fiber length attrition during surface machining. While this fiber attrition negatively impacts the mechanical performance of the material in the print direction, it seems that the changes in processing behaviors and print quality, namely the surface roughness of the printed structure associated with shorter fiber lengths, is beneficial to interlayer adhesion. The tensile strength and elastic modulus of the recycled material, in the print direction, decreased 11% and 31% respectively compared to the pristine material. However, in the layer-wise direction it was found that the recycled material exhibited no significant change in elastic modulus and a significant 21% increase in tensile strength – a surprising result. This work indicates that machining waste could be a viable material stream for recycled LFAM feedstock materials.

1. Introduction

Composite materials, such as carbon-fiber reinforced polymers (CFRPs), are industrially desirable materials due to their high-strength-to-weight ratio and durability in multiple manufacturing industries [1–4]. For example, CFRPs have seen widespread adoption in commercial aircraft (e.g., Boeing 787) and rapid production and prototyping for the mold/tooling industry [5–7]. The demand for composite materials, specifically thermoplastic composites, is expected to have a compound annual growth rate of 6.9% in the US market between the years 2022–2030, where the primary demand is for short discontinuous fiber composites [8] as driven by the growth of the aerospace, marine, and wind energy application sectors [9–12].

New manufacturing processes for short fiber CFRPs, like large-format additive manufacturing (LFAM), are growing rapidly and use high volumes of CFRPs [1,13]. Although CFRPs are expensive and carbon-intensive materials, the addition of short discontinuous carbon fiber (CF) to polymers reduces warpage during the printing process while simultaneously increasing the mechanical performance of the printed structures; these benefits make them necessary for the large-scale printing of some high-performance applications [4,14]. The Big Area Additive Manufacturing (BAAM) system, developed by Oak Ridge National Laboratory (ORNL) and Cincinnati Inc., is an LFAM system capable of producing significantly larger parts than traditional benchtop AM technologies, partially enabled using a high-throughput single-screw extruder and pelletized material, such as carbon fiber acrylonitrile butadiene styrene (CF-ABS), as a feedstock [4,15,16]. LFAM and CFRP feedstock materials have been critical to developing rapid mold and tooling production – especially for low-volume, high-value tooling components. For example, the BAAM system has been used to manufacture a catamaran boat hull mold, which was 10.36 m in length and required the use of 2494.76 kg of material [1]. As the demand

* Corresponding author.
E-mail address: koreym@ornl.gov (M. Korey).

https://doi.org/10.1016/j.compositesb.2024.111291
Received 22 November 2023; Received in revised form 24 January 2024; Accepted 4 February 2024
Available online 9 February 2024

for thermoplastic composites increases, notably driven by industries such as LFAM mold/tooling, production scrap and end-of-life composite materials are also expected to increase significantly.

As demand for LFAM feedstocks grows, a robust and sustainable supply chain of CFRPs must be available [23]. As supply chain issues remain an industrial concern, some are looking to use recycled materials to bolster the supply of pristine feedstock material. However, the recycling of composites and their filler materials has yet to see broader market adoption, likely due to composite performance degradation, as recycled materials can exhibit lower mechanical properties when compared to their pristine counterparts [17–20]. In addition, recycling fiber-filled composites poses a particular challenge due to the increased complexity of the fiber-matrix interface and varied microstructural composition [21,22]. Mechanical recycling, the process of size-reducing bulk materials either through grinding/granulation or other mechanical means such as milling [23], is an emerging technique for recovering high-value composite materials from LFAM end-of-life parts with minimal impacts on mechanical performance, thereby mitigating the energy demand and cost associated with these feedstocks [6,17,24]. Recent studies on the utilization of granulated feedstock materials for LFAM have demonstrated the viability of using recycled fiber-filled materials in LFAM parts such as pre-cast concrete molds [17,24,25]. Recycled thermoplastic composites have also been utilized in the development of urban furniture [26] and automotive parts, such as an aerodynamic splitter mold [27]. In addition to recycling end-of-life waste, it was found that up to 40% of CFRP waste (inclusive of all CFRP manufacturing) is generated as processing scrap in the manufacturing stage, before the first application life of the manufactured part [12]; it is estimated that approximately 7000–15,000 tons of processing waste is generated each year [23]. This scrap is an un-tapped material stream consisting of potentially high-value CFRP materials.

In LFAM, waste generation occurs at every step of the manufacturing process – especially in the surface finishing of parts. To achieve geometric tolerances and a uniform surface finish, LFAM parts undergo surface machining, a subtractive process resulting in high volumes of small, flake-like particles and off-cuts that are typically landfilled. When considering the viability of utilizing machining scraps as recycled feedstock materials, understanding how material degradation may affect resulting properties is critical. There are two major aspects of degradation that must be considered: (1) how the recycling and remanufacturing process affect the matrix phase of the material (*e.g.*, molecular weight degradation) and (2) how the recycling and remanufacturing process affect the fiber phase of the material (*e.g.*, fiber loss or attrition).

ABS is an amorphous co-polymer that has been shown to degrade via a chain-scission mechanism in the presence of high thermal and mechanical energy, like what would be experienced in the milling and repelletization process [28,29]. Chain scission causes the breaking of bonds and has been shown in ABS to produce low molecular weight oxidation products, resulting in a lower molecular weight, and in some instances the formation of stable cross-linked structures [30]. A reduction in molecular weight has been associated with decreased thermal properties, decreased viscosity, and decreased mechanical properties, due to the changes in the way in which the polymer chains are able to entangle with each other – where less entanglement has been directly correlated to a reduction in mechanical performance [31]. In a previous study Bai et al. [32] investigated the degradation behavior of ABS that had been processed three times on a torque rheometer at 230 °C. They found that there were minimal degradation effects on the polybutadiene (PB) and styrene-acrylonitrile (SAN) phases of the ABS. However, they also found that when ABS is re-processed at a higher temperature, 290 °C, there was significant thermo-oxidative degradation that occurred due to crosslinking reactions in the PB-phase of the ABS after three cycles.

As CF-ABS is a short fiber composite material, it is also important to consider the potential for degradation of the fiber-phase of the material. As discussed above, the machining and repelletization process are mechanically intensive, with potential for fiber attrition at either the milling process or the high shear/high extensional flow deformation during the twin screw re-pelletization process [33–35]. Fiber attrition is a primary concern in the recycling of composites [12], as reductions in fiber length can also cause reductions of viscosity, changes in fiber orientation that would affect thermomechanical properties such as the coefficient of thermal expansion, and reductions in bulk mechanical properties such as tensile strength and modulus. Quantifying material degradation from this industrial process and elucidating its underlying mechanism is critical to the industrial adoption of this recycled feedstock.

Machining and processing scrap could provide a sustainable and economical feedstock to the LFAM and CFRP industry, however, further investigation is necessary to understand the value and the viability of recycling these materials. This recycling approach is not without its

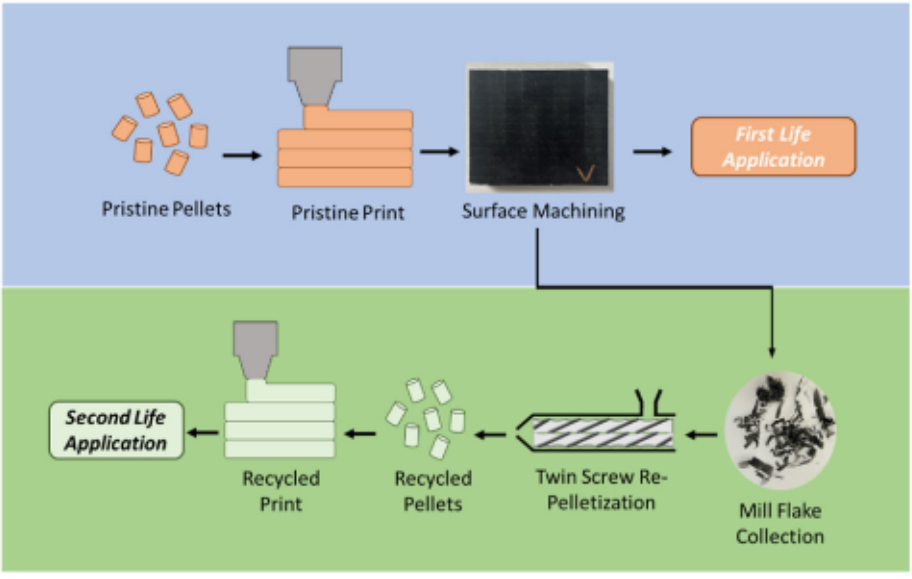

Fig. 1. An overview of the recycling process is shown where the material's first and second life is shown in the blue and green background, respectively. (For interpretation of the references to color in this figure legend, the reader is referred to the Web version of this article.)

challenges; for example, the collection of machining waste poses difficulty in the recycling process due to the shape and size of the material and the potential for contamination. Herein, the potential for recycling CF-ABS material scrap generated during the surface finishing of LFAM parts was investigated (Fig. 1). By repurposing machining scrap, we aim to demonstrate its potential as a recycled LFAM feedstock material, resulting in environmentally sustainable parts, reduced demand for pristine CFRP materials, and the creation of a value-added process for CFRP waste materials.

2. Materials and methods

Pristine CF-ABS pellets were utilized as the starting material for this study. Techmer PM (Clinton, TN) provided the Electrafil ABS 1501 3DP with 20 wt% short carbon fiber (CF). The recycled CF-ABS was produced from machining scraps in the form of flaked particles (*i.e.*, mill flakes) from subtractive surface machining processes, specifically large-scale computer numerical control (CNC) and bench top scale CNC machining, of printed structures. These mill flakes (cf. Fig. 1) were compounded and repelletized by Techmer PM via twin-screw extrusion (TSE).

2.1. Printing

Pristine CF-ABS and recycled CF-ABS pellets were printed on the BAAM system at ORNL's Manufacturing Demonstration Facility (MDF). The materials were dried at 80 °C for 4 h prior to printing. The pristine and recycled pellets were printed at 250 °C and 45 RPM, with a 0.76 cm nozzle diameter and a 90-s layer time to achieve 24" x 24" x 12" boxes. The printed samples were allowed to cool for 15 min on the print bed, maintained at 100 °C, before removal to reduce part warpage.

2.2. Gel permeation chromatography

The molecular weight distribution of neat ABS pellets, pristine and recycled pellets, mill flakes, and the pristine and recycled prints were measured using gel permeation chromatography (GPC), a type of size exclusion chromatography (SEC). Neat ABS was utilized in this experiment as a comparison material as it is the base matrix of the materials of interest. The materials were dissolved in tetrahydrofuran (THF) with magnetic stirring. The resulting solutions were then filtered to remove fiber from the solutions and distributed into high-performance liquid chromatography (HPLC) vials. THF was used as the mobile phase at a flow rate of 1.0 mL/min. The GPC process was completed with an Agilent 1260 Infinity II. Reported molecular weight values were acquired via conventional calibration analysis using polystyrene standards over the range of 1000 g/mol to 1,000,000 g/mol.

2.2.1. Thermogravimetric analysis

A TA Instruments Discovery series thermogravimetric analyzer (TGA) was used on neat ABS pellets, pristine and recycled pellets, mill flakes, and the pristine and recycled prints to understand the degradation mechanisms of the CF-ABS. A temperature ramp from 30 °C to 600 °C with a heating rate of 10 °C/min was completed for all sample types in both an air and argon environment. A triplicate was run for all sample types. The decomposition temperature was measured at 2 wt% and 5 wt% loss to determine thermal stability. The final mass of each sample type at 600 °C was recorded to quantify the fiber amount in the composite and determine if any fiber was lost during the recycling or printing processes.

2.3. Fiber length analysis

Microscopy was utilized to image the fibers from pristine and recycled pellets, mill flakes, and the pristine and recycled print (Fig. 1). In order to isolate the carbon fiber from the polymer matrix, ultrasonic-aided digestion was utilized [36], using acetone as the solvent. Approximately 3–5 g of material samples, either pellet, flake, or small print samples recovered with a chisel, were mixed with approximately 50 mL of acetone. The solutions were placed in an ultrasonic bath and allowed to sonicate for at least 90 min at room temperature. The resulting solutions were then applied to microscopy slides, given time for the acetone to evaporate from the slide surface, and imaged on a Keyence Optical Microscope with 50x total magnification. The images were processed and measured using ImageJ [37]. The lengths of the fibers were then measured, excluding unclear, incompletely imaged, or overlapping fibers. A minimum of 1500 fibers were imaged and measured for each sample. The results were analyzed for statistical significance ($p < 0.05$), and their distributions were observed using a log–normal distribution analysis [38]. Weighted average fiber length was used to report the average fiber length of each sample [39].

2.4. Rheological characterization

The rheological behavior of neat ABS pellets, pristine and recycled pellets, mill flakes, and the pristine and recycled prints were measured using a Discovery Hybrid Rheometer-2 (DHR-2), using a parallel plate geometry with a diameter of 25 mm. The rheological testing was performed at 250 °C, which is the BAAM printing nozzle temperature for pristine CF-ABS. The materials were exposed to an oscillatory frequency sweep in air at a frequency range of 0.1–628 radians per second and applied strain of 0.1 %. The frequency ranges were chosen to simulate the shear rate range of material within the printing nozzle and at the nozzle exit. The applied strain was chosen to fall within the materials' linear viscoelastic region. The gap height between the plates was 1.5 mm. The materials were dried at 80 °C for 4 h prior to testing.

2.5. Density measurements

The density of the pristine and recycled CF-ABS pellets, the mill flakes, and the pristine and recycled prints were measured using a Micromeretics AccuPyc 1340 gas pycnometer. Sample weights ranged from ~0.4 g (flakes) to ~2.5 g (printed samples). Each sample was dried and allowed to cool prior to testing. The mass of each sample was recorded prior to placing in the system. The sample was sealed in the testing chamber and was flooded with Helium gas and allowed to reach equilibrium to rapidly fill sample pores and then was discharged into a second chamber and allowed to reach equilibrium to calculate the solid phase volume of each sample. One sample was used to acquire 5 density measurements and used to determine the average density of each material.

2.6. Surface roughness characterization

Due to noticeable differences in the surface finish of the recycled print compared to the pristine print (cf. Fig. 2), the topology and surface roughness of the surface of each printed sample was investigated. Using a Keyence VR-5000 Wide Area 3D Measurement System, a non-contact

Fig. 2. Surface imaging is provided for the pristine (left) and recycled (right) printed parts.

profilometer, 15 mm × 30 mm samples from each printed structure were scanned at 40X high-definition magnification. After scanning, five 3 mm × 7 mm surface roughness measurements were observed using area scans and quantified using Keyence VR-5000 analysis software. These values were averaged and tested for statistical significance ($p < 0.05$). In addition to surface roughness, surface topology was visualized. Each printed sample was normalized to the flat scanning plate for surface topology visualization and is only used as a qualitative aid in understanding the difference in surface finish as a function of recycling.

2.7. Digital image correlation for thermomechanical properties

Thermomechanical properties of LFAM materials can be characterized using 2D digital image correlation (DIC) by using a unique speckle pattern to track the movement of entire surfaces before and after thermal loading [40,41]. The Digital Image Correlation Oven (DIC Oven) is a technique that was developed to characterize coefficient of thermal expansion (CTE) experienced by an LFAM structure by using DIC as a global method to measure thermal-induced strain [42]. Printed pristine and recycled samples for this work were prepped for DIC Oven testing by machining the face of interest to a flat surface. The LFAM structures were then dried at 80 °C for 8 h. The machined face of interest was then coated with a thin layer of matte white colored high-temperature Krylon spray paint and covered in black ink speckles to create a clear contrast of unique points for accurate DIC measurements. The sample was positioned, tested at room temperature to provide baseline positions of the speckles, and tested at an elevated (steady state) temperature of 90 °C using the DIC Oven as explained in previous literature [42]. The room temperature and steady state temperature images were uploaded to Correlated Solutions' Vic-2D software to calculate the thermal-induced strains experienced by the sample. The known temperature states, calculated room temperature strains, and calculated steady state strain were used to calculate CTE of the LFAM structures using the method described in this authors previous work [42]. The DIC Oven is a global technique that better represents thermomechanical properties of LFAM structures than by traditional, local techniques such as thermomechanical analysis (TMA) due to the complex microstructure of printed parts [42].

2.8. Mechanical characterisation

Mechanical properties (*i.e.*, Young's elastic modulus and the ultimate tensile strength (UTS)) of the pristine and recycled prints were measured to determine the influence of the recycling process on mechanical performance. Five tensile samples were cut from both the X and Z directions (Fig. 2) to determine the changes in tensile strength in the printing direction (X-direction) and also to observe the layer-layer strength of the normal direction (Z-direction). The tensile specimens were water jet cut from machined walls from each printed sample to ASTM D638 Type 1 size specifications. The tensile testing was completed at a rate of 5 mm/min on an MTS Criterion Series, Model 45, with a 10 kN load cell, and extension was measured using an MTS LX 500 Laser Extensometer.

3. Results and discussion

3.1. Effect of recycling on matrix phase and fiber reinforcement

To determine any degradation impacts on the matrix phase, the molecular weight of CF-ABS, as a function of recycling, was observed with GPC analysis (cf. Fig. 3 and Table S2). As the machining and repelletization processes are mechanically and thermally intensive, potentially leading to chain scission in the matrix phase, monitoring the molecular weight as a degradation indicator allows for a better understanding of the potential degradation of bulk mechanical properties. Due to the primary shape of machining waste being flake-like particulate, it must be compounded into pellets prior to printing, introducing an additional thermo-mechanical cycle before printing, potentially increasing the likelihood of polymer degradation. It was important to observe the molecular weight at each step of the conversion and printing process in order to understand how stable the materials were after each thermo-mechanical cycle as reductions in molecular weight can result in reductions in mechanical properties [43]; specifically, if the molecular weight decreases below the critical weight of entanglement, it can cause a reduction in tensile strength, modulus, and glass transition temperature due to a reduction in entanglement between chains [44]. No significant ($p > 0.05$) reduction in molecular weight was recorded as a result of either the recycling or printing process. In addition to no significant decrease in molecular weight, it was also observed that there was no significant change in polydispersity index (PDI), indicating that the recycled material is as heterogeneous in molecular weight as the pristine material. Based on these results, there is no indication that the molecular weight of the recycled material would contribute to a reduction of mechanical properties or thermal behavior. As further confirmation of the minimal reduction in molecular weight and the effect on thermal properties, differential scanning calorimetry (DSC) was performed and confirmed that there was no significant change in glass transition temperature (T_g) as a function of the recycling or printing process (Figure S1 and Table S1). The degradation profiles of the recycled materials were also observed with TGA after each step in the recycling and printing process (Table S3), there was no significant ($p > 0.05$) difference in the material weight at the print deposition temperature of the recycled pellets compared to the pristine pellets.

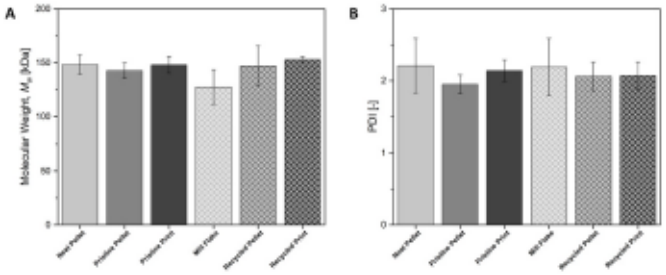

Fig. 3. GPC results for the materials of interest: A) weighted average molecular weight (M_w) and B) polydispersity index (PDI); the results show that there is no significant change in M_w or PDI in the recycled CF-ABS samples compared to the pristine CF-ABS.

After confirming there was no significant molecular weight reductions, the fiber reinforcement phase was explored as a function of recycling and printing to understand potential degradation mechanisms that could influence mechanical performance. In the collection of machining scraps, there were concerns that fiber content would be reduced due to the generation of small flake-like particulates and dust that may be unable to be reclaimed prior to repelletization, potentially decreasing the fiber weight content below 20 wt%. To determine the fiber weight content of each sample, TGA was performed in an inert

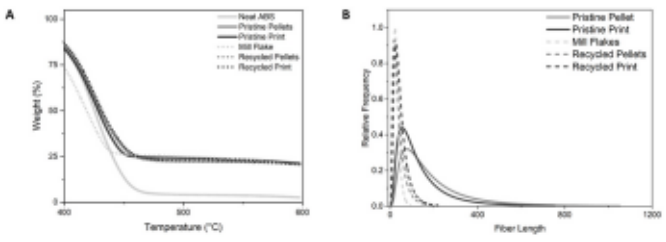

Fig. 4. A) Carbon fiber content as measured via TGA at 600 °C. There is no significant change in residual fiber content compared to the pristine CF-ABS materials. B) Fiber length analysis of all samples is visualized using a log normal distribution. A significant reduction in fiber length was observed, with the most significant reduction occurring after the surface machining process.

environment to quantify the residual fiber content at 600 °C (Fig. 4A). After comparing the remaining fiber content of the pristine print (18.53% ± 0.5) to the recycled print (17.09% ± 0.3), no significant ($p > 0.05$) difference in fiber weight percentage was observed after recycling (Table S3).

After confirming the fiber content was minimally impacted, the average fiber length was then explored at each step of the recycling process and the individual measurements were visualized using a log-normal distribution (Fig. 4B). Preserving fiber length in short fiber composites is important in the preservation of mechanical properties after the recycling and remanufacturing process. Composites with fiber lengths greater than the critical fiber length (CFL), the minimum fiber length necessary for maximum reinforcement, exhibit superior performance compared to systems with fiber lengths less than the CFL [45,46]. The documented CFL for short discontinuous CF-ABS is ~3 mm [47]. The average fiber length of the collected mill flakes was compared to the average fiber length of the pristine print to determine the effect the machining process has on fiber attrition; it was observed that the average fiber length of the mill flakes (45 μm) was 80% shorter than that of the pristine print (226 μm) after the machining process. This average is relatively stable during the TSE conversion and printing steps, indicating that the machining process is the step in which the most fiber degradation occurs. Further, 91% of the measured fibers within the recycled CF-ABS printed material were less than or equal to 100 μm compared to 44% in the pristine CF-ABS print, which is visualized in Fig. 4B.

It is important to note that fiber length directly affects the load transfer process, which has been widely researched for short fiber composite materials as documented in previous literature [39,48,49]. The pristine print and recycled print have an average fiber length that is far below the documented CFL, where the pristine print's and recycled print's average fiber length is 93% and 96% shorter than the documented CFL, respectively. Therefore, it is expected that while both materials are unable to achieve maximum load transfer [21,45,49,50], the pristine material should exhibit higher mechanical properties than the recycled material. As the molecular weight and fiber content are not significantly changing while the average fiber length is reduced significantly, we postulate that fiber attrition during the machining process is the primary mechanism for any observed reduction in the bulk mechanical properties of the recycled material.

3.1.1. Effect of recycling on processability and print quality

Beyond the anticipated impacts to mechanical performance, it is expected that the significantly reduced fiber length will also impact the composite processing, notably the complex viscosity in relationship to angular frequency [51–55], as reported in Fig. 5. Complex viscosity of LFAM feedstocks is important as the viscosity directly impacts the shear experienced by the material in the nozzle during deposition and therefore fiber alignment in the printed structure. The recycled CF-ABS pellets exhibit an overall decreased complex viscosity; at ~100 s^{-1}, the approximate shear rate at the nozzle exit [14], the recycled CF-ABS shows a 97% decrease in complex viscosity when compared to the pristine CF-ABS pellets and a 41% increase in complex viscosity when compared to neat ABS. Due to there being no significant change in molecular weight or fiber content, we propose that the degradation of complex viscosity is directly related to the degradation of fiber length (Figure S2). At low shear rates, the effect of fiber attrition is more pronounced than at high shear rates, this phenomena is consistent with previous literature [52,56].

Fiber length impacts the composite rheology and subsequent printing conditions as visibly noticed on the surface finishes of the pristine and recycled prints, where the recycled print was significantly smoother (cf. Fig. 2). To quantify the change in average surface roughness, profilometry scans were completed for each print surface where 3D height maps of the surface topology are visualized for each print in Fig. 6.

Utilizing area scans, the surface roughness of the printed structures

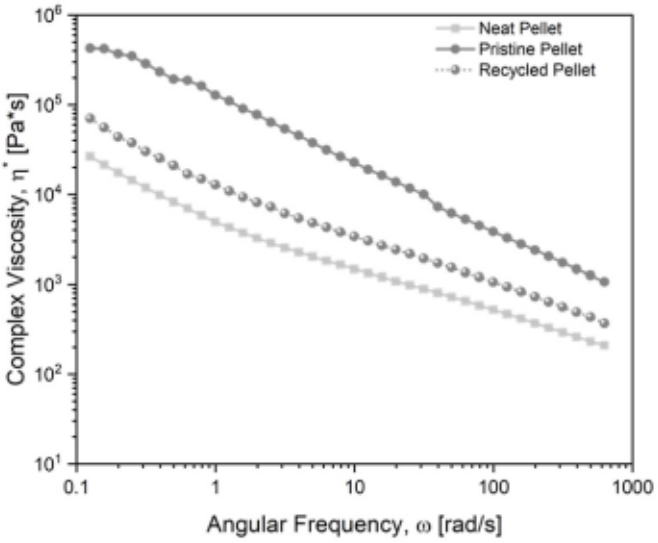

Fig. 5. Frequency sweeps were utilized to observe the complex viscosity of the pristine and recycled pellets to characterize the effect of recycling on flow properties. Neat ABS is used as a comparison to illustrate the substantial reduction in complex viscosity compared to the pristine composite material.

was characterized, where the recycled print was found to exhibit a 19% decrease in surface roughness compared to the pristine print. It is not uncommon for additively manufactured structures to exhibit poor surface finish, namely surface roughness, and is a result of the processing conditions of the material. Previous literature has identified that the increased fluidity of the deposited material results in smoother surface finish [57] and that materials exposed to lower shear rates during deposition have more uniform surface features [58]. Increased fluidity during printing is most often controlled by the deposition temperature; in this study the recycled materials exhibit an increased fluidity due to the resulting decreased viscosity (cf. Fig. 5) and shear rates during extrusion due to fiber attrition rather than a change in processing temperature. The significant reduction in surface roughness could potentially have a direct effect on the mechanical performance of the printed structures, specifically the z-direction tensile strength, as a change in surface roughness could influence the interlayer bonding.

Further, the density of the printed samples was measured to determine if the recycled material exhibited decreased density, which would be indicative of increased concentrations of porosity within the structure. Print density has been shown to directly affect mechanical performance, where reduced print density often causes a reduction in bulk mechanical properties like tensile strength. Density, measured via gas pycnometry of printed pristine and recycled samples, confirms that there is also no significant change in print density when comparing the recycled and pristine printed materials (Figure S3). Based on these results, it is not anticipated that density will influence the final bulk mechanical properties.

3.1.2. Effect of recycling on print performance

As previously discussed, the addition of short CF to polymer feedstocks used in LFAM applications reduces warpage that occurs during printing. During printing, deposition of material can result in part warpage due to the thermal conditions during printing and the thermomechanical properties of the material itself. Mitigating and reducing part warpage in LFAM materials is critical to ensuring that the print head does not collide with the part during the deposition process and that the final structure is geometrically accuracy [14]. Therefore, the CTE of the recycled CF-ABS printed structure was measured and compared to the pristine CF-ABS printed material with the use of a DIC oven (Table 1). It was observed that there was a significant increase (60%) in the

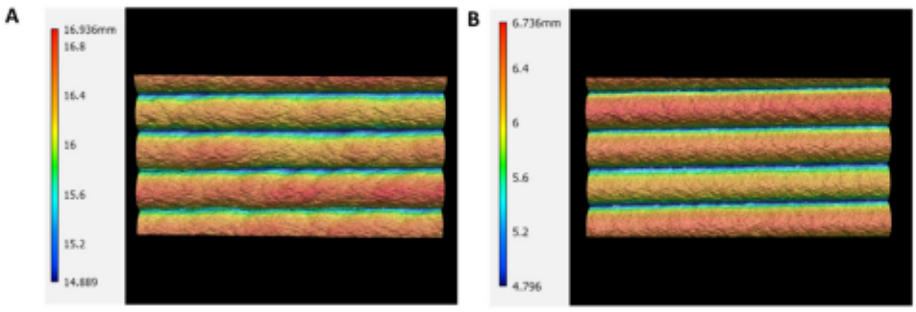

Fig. 6. Height map visualization of the printed surface topographies. A) Surface topography of pristine CF-ABS (Surface Roughness = 239.4 ± 12.6 μm) and B) surface topography of recycled CF-ABS (Surface Roughness = 193.5 ± 4.9 μm). There was a significant decrease ($p < 0.05$) in surface roughness of the recycled print compared to the pristine sample.

Table 1
Average CTE values for each printed structure where significant change ($p < 0.05$, denoted via *) is seen in both directions of the recycled print when compared to the pristine print.

Material	X-Dir [μm/m°C]	Z-Dir [μm/m°C]
Pristine Print	27.51 ± 1.04	126.75 ± 4.25
Mill Flake Print	43.99 ± 1.02*	117.60 ± 3.26*

x-direction CTE (CTE_X) when comparing the pristine printed structure to the recycled printed structure and a significant reduction (7%) in the z-direction CTE (CTE_Z), as visualized by the strain contour plots in Fig. 7.

The strain contour plots created using Vic-2D visually represent the thermal-induced strains experienced by the LFAM structure at steady state heating conditions. Fig. 7A and B visually represent the thermal induced strain experienced in the x-direction of the pristine and recycled printed samples, respectively. The x-direction strain contour plots show low, homogenous strain values for both the pristine and recycled material; while the strain maps are homogenous in both cases, it is worth noting that the strain values are nearly double for the recycled material in comparison to the pristine material. Homogeneity of strain in the x-direction was expected as the reinforcement material is postulated to be aligned in this direction during printing and the fiber best resists expansion in this direction. However, these results indicate that the fibers in the recycled sample are unable to resist expansion as well as the pristine material. Duty et al. [14] showed that dimensional stability of LFAM parts, such as the propensity of detrimental part warpage, was directly related to the CTE of the material in the print direction. It was found that neat ABS, which has a reported CTE of ~100 μ/m/°C, was much less dimensionally stable at large structural ratios than CF-ABS with a CTE of ~19 μ/m/°C [14,59]. An increase in CTE_X would increase thermal expansion/contraction during printing causing potentially detrimental warpage at increased structure sizes, in-situ collisions between the print head and the printed structure, and unusable printed parts [14]. Due to the increase in CTE_X observed in this study, the printability of this material may be limited, specifically the maximum print size.

In previous literature, CTE has been shown to be influenced by the orientation of fibers within a printed structure [22], where CTE values are the lowest at highly oriented regions (*e.g.* the bead edge) and highest in regions with more random fiber orientation (*e.g.* the center of the bead). Utilizing the DIC Oven and strain contour plots, the potential change in fiber orientation can be indirectly observed. In Fig. 7C and D, the z-direction contour plots highlight the influence of fiber orientation on the thermomechanical performance of the print. The red bands that represent high strain regions are present at the interface of layers where highly aligned edges of beads meet. As short carbon fibers poorly resist thermal loading in this direction, perpendicular to alignment, this

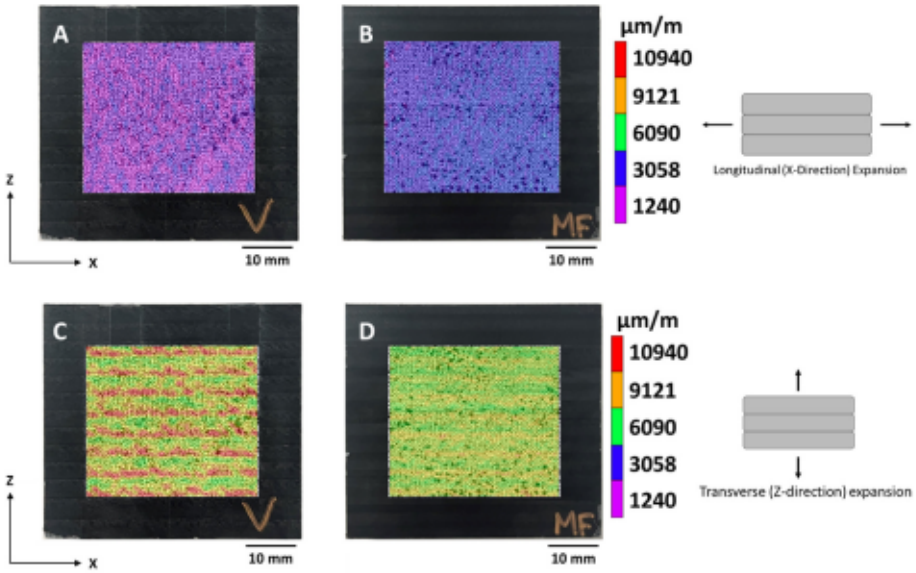

Fig. 7. Strain contour plots captured through DIC measurements. A and B) Visualization of strain in X-direction strain for pristine and recycled CF-ABS. C and D) Z-direction visualization for pristine and recycled CF-ABS. There was a significant increase in CTE_x and a significant decrease in CTE_z when compared to the pristine print.

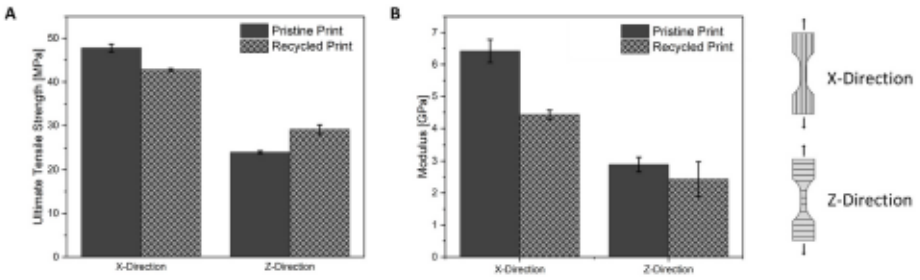

Fig. 8. The UTS (A) and tensile modulus (B) of the X- and Z-directions of printed pristine CF-ABS and recycled CF-ABS. Schematics are provided (right) to illustrate the directionality of the mechanical properties.

causes high regions of strain (red) at layer interfaces in the z-direction plots. The regions of relatively low strain bands (green) are representative of the more randomly oriented fiber at the center of the bead. The red banding phenomena is noticeably absent in the z-direction strain contour plot of the recycled material, where the edge region is instead characterized by a lower strain represented by yellow-green banding at layer interfaces. The contour plots suggest a reduction of fiber alignment in the direction of the print (x-direction) in recycled samples; further verification of this phenomena could potentially be observed by a reduction in the x-direction mechanical performance.

In order to observe the impact of utilizing recycled CF-ABS made from machining waste (i.e., mill flakes) on the resulting mechanical properties, the tensile strength and modulus were measured and compared to the pristine CF-ABS samples (Fig. 8). In the printing direction (x-direction), the average tensile strength and modulus of the recycled prints decreased 11% and 31% respectively ($p < 0.05$), compared to the pristine prints. A reduction in x-direction mechanical properties is consistent with previous literature on CF-ABS recycling for LFAM [17] and can be attributed to changes in the microstructure of the printed part, corroborated by the reduction in fiber length observed in this work. However, perpendicular to the print direction (z-direction), the recycled print displayed a 21% increase in tensile strength ($p < 0.05$) with no significant change in modulus when compared to the pristine material. This is surprising as in AM structures, the z-direction strength is often much lower than the x-direction strength due to: 1) the interlayer adhesion forces being weaker than the cohesive forces within a bead, and 2) the reduction of fiber alignment, where fibers are typically more aligned in the print direction due to shear experienced in the nozzle during the printing process [17,60], resulting in mechanically anisotropic structures. Increasing z-strength has seldom been observed and represents a known weakness in many additive manufacturing processes, yet in the present study, the utilization of machining waste as LFAM feedstock significantly enhanced the z-strength of the printed structure. To the best of the authors' knowledge, this is the first time that an increase in z-strength has been observed in a recycled material for LFAM applications.

To explore the unexpected increase in z-direction strength with recycling, it is critical to understand how material changes impacted its processing and affected the bonding quality between layers. For amorphous polymers, like ABS, the primary mechanism of bonding is viscous sintering where bond coalescence occurs instantaneously after surface contact [61,62]. Once in contact, the bond strength will increase until the temperature of the material falls below the glass transition temperature, as molecular mobility across beads becomes inhibited [63]. Increased rates of coalescence have been directly related to lower material viscosities and increased interlayer strength [60]. It is postulated that the reduction in fiber length, previously noted, is the primary relevant material change throughout processing, where the reduction in fiber length is the reason for the reduction in viscosity of the recycled materials.

It is important to note though, that the area of contact must be considered when assessing bond quality as bond coalescence can only occur when the deposited material is in contact with a substrate material [60,64]. Due to microstructural defects that occur during deposition, a widely known limitation of AM, contact area may be limited. Discussed in a previous section, the viscous properties of a material during deposition directly impact the surface finish of a printed structure, where the recycled material exhibited both a decreased viscosity and a significantly lower surface roughness. It is reasonable to assume that the decreased viscosity and surface roughness observed in the recycled

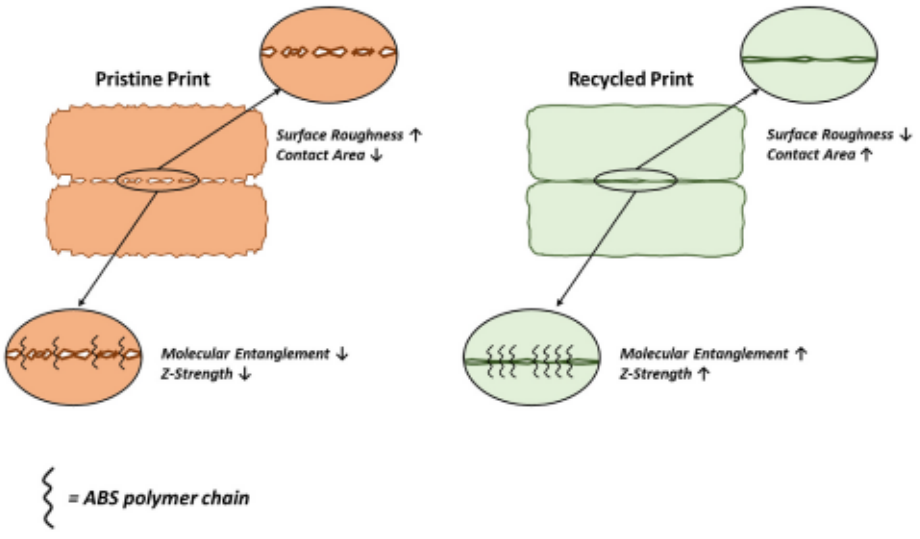

Fig. 9. Proposed mechanism for increased z-direction strength of the recycled material as a function of print surface roughness.

material allowed for an increased contact area between print layers. This increased surface area of contact between print layers would allow for better molecular diffusion and increased molecular entanglements between the substrate layer and the depositing layer [31], leading to an increased z-direction strength as observed in Fig. 8A. This proposed mechanism is illustrated in Fig. 9. It should be noted that while the print density of the recycled material was not significantly different from the pristine material, the location and size of voids at the interface may also contribute to the available contact area for bonding and will be considered in future work. Further work is still needed to investigate and validate the role that surface roughness plays in the contact area between layers and ultimately the mechanism by which interlayer adhesion occurs in the recycled printed structure.

4. Conclusions

In summary, this study demonstrated the successful recycling and utilization of CF-ABS machining scraps as an LFAM feedstock. The primary degradation mechanism was determined to be the significant fiber length attrition that occurred during the surface machining process, where there was an 80% reduction in average fiber length. The recycling and printing process showed no significant effect on the molecular weight or the fiber content of the recycled material. Both the pristine and recycled materials were printed under the same conditions, but the recycled material displayed a significant 97% reduction in viscosity from the pristine material, which can be attributed to the reduction in fiber length. Reductions in viscosity during processing reduce the shear rates experienced during extrusion, potentially resulting in decreased fiber orientation in the x-direction (printing direction) of the part. Though fiber orientation was not directly measured in this study, orientation effects in printed structures can be observed through visualization of strain using x- and z-direction contour plots when measuring CTE. This study identified a significant increase in CTE_X (60%) and a significant decrease in CTE_Z (7%), where the strain contour plots in the x-direction show homogeneous strain in the recycled print twice that of its pristine counterpart. The orientation effects are most noticeable in the z-direction contour plots, where decreased visualized strain, typically associated with increased random orientation of fibers, was observed in the recycled print. A future area of study will be focused on characterizing the changes in microstructural composition due to utilization of recycled feedstock materials, specifically the direct effect on fiber orientation.

As a result of the changing microstructure, the recycled print in the x-direction exhibited reductions of both tensile strength and modulus, 11% and 31% respectively, when compared to the pristine print. A particularly significant finding, however, was the unexpected 21% increase in z-direction tensile strength when compared to the pristine print. As discussed, the reduced fiber length in the recycled material resulted in a decreased complex viscosity, influencing the interlayer bonding mechanism in the recycled print. It was found that the recycled print had a significantly lower surface roughness compared to the pristine print, potentially increasing the amount of contact area for bonding during deposition. These findings indicate that both the viscosity during deposition and the amount of available contact area for bonding play a role in the observed z-direction tensile strength increase. Future work will focus on investigating the influence of surface roughness and the role it plays in interlayer adhesion. Herein, this study shows the successful recovery, recycling, and utilization of CF-ABS machining waste as an LFAM feedstock and highlights a previously unutilized material sources' industrial viability. This study also highlights broader implications for the use of processing waste as a material source for more sustainable material development and maintaining a robust supply chain for the composite manufacturing industry.

CRediT authorship contribution statement

Roo Walker: Writing – original draft, Visualization, Methodology, Investigation, Formal analysis, Conceptualization. **Matthew Korey:** Writing – review & editing, Methodology, Investigation. **Amber M. Hubbard:** Writing – review & editing, Methodology, Investigation. **Caitlyn M. Clarkson:** Writing – review & editing, Methodology, Investigation. **Tyler Corum:** Writing – review & editing, Methodology, Investigation, Formal analysis. **Tyler Smith:** Methodology. **Christopher J. Hershey:** Methodology. **John Lindahl:** Methodology. **Soydan Ozcan:** Writing – review & editing, Supervision, Project administration, Funding acquisition. **Chad Duty:** Writing – review & editing, Supervision, Project administration, Funding acquisition.

Declaration of competing interest

The authors declare that they have no known competing financial interests or personal relationships that could have appeared to influence the work reported in this paper.

Data availability

Data will be made available on request.

Acknowledgments

The US Department of Energy (DOE), Office of Energy Efficiency and Renewable Energy, Advanced Materials and Manufacturing Office provided support for this work under CPS Agreement 35863. The authors would like to acknowledge the Sustainable Materials and Manufacturing Alliance for Renewable Technologies Consortium, as well as the Manufacturing Demonstration Facility of Oak Ridge National Laboratory. The authors would also like to thank Techmer PM for providing material and completing the compounding of the collected materials for recycling. The authors would like to thank Jake Dvorak and the University of Tennessee MABE Maker Lab for assisting in machining and sample preparation. The authors would like to thank the following people and research groups for access to equipment and assistance in sample preparation: Evan Holt and the Kilbey Lab at the University of Tennessee, Matthew Roach and Dr. Bradley Jared at the University of Tennessee, Sarah Graham at Oak Ridge National Laboratory, and Ally Collier and Nina Bhat from the PCAM Lab at the University of Tennessee.

Appendix A. Supplementary data

Supplementary data to this article can be found online at https://doi.org/10.1016/j.compositesb.2024.111291.

References

[1] Post BK, Chesser PC, Lind RF, Roschli A, Love LJ, Gaul KT, et al. Using Big Area Additive Manufacturing to directly manufacture a boat hull mould. Virtual Phys Prototyp 2019;14:123–9. https://doi.org/10.1080/17452759.2018.1532798.
[2] Post BK, Richardson B, Lind R, Love LJ, Lloyd P, Kune V, et al. Big area additive manufacturing application in wind Turbine molds. University of Texas at Austin; 2017. https://doi.org/10.26153/tsw/16964.
[3] Roschli A, Gaul KT, Boulger AM, Post BK, Chesser PC, Love LJ, et al. Designing for big area additive manufacturing. Addit Manuf 2019;25:275–85. https://doi.org/10.1016/j.addma.2018.11.006.
[4] Duty CE, Drye T, Franc A. Material development for tooling applications using big area additive manufacturing (BAAM). Oak Ridge National Lab. (ORNL), Oak Ridge, TN (United States). Manufacturing Demonstration Facility (MDF) 2015. https://doi.org/10.2172/1209207.
[5] Billah KMM, Heineman J, Mhatre P, Roschli A, Post B, Kumar V, et al. Large-scale additive manufacturing of self-heating molds. Addit Manuf 2021;47:102282. https://doi.org/10.1016/j.addma.2021.102282.
[6] Armstrong KO, Kamath D, Zhao X, Rencheck ML, Tekinalp H, Korey M, et al. Life cycle cost, energy, and carbon emissions of molds for precast concrete: exploring the impacts of material choices and additive manufacturing. Resour Conserv Recycl 2023;197:107117. https://doi.org/10.1016/j.resconrec.2023.107117.

[7] Duty CE, Kunc V, Lokitz BS, Springfield RM. Evaluation of additive manufacturing for high volume composite Part Molds. Oak Ridge National Lab. (ORNL), Oak Ridge, TN (United States). Manufacturing demonstration facility (MDF). 2017. https://doi.org/10.2172/1360075.

[8] Global thermoplastic composites market size report. 2024. n.d, https://www.grandviewresearch.com/industry-analysis/thermoplastic-composites-market-report. [Accessed 17 March 2023].

[9] Fallon JJ, McKnight SH, Bortner MJ. Highly loaded fiber filled polymers for material extrusion: a review of current understanding. Addit Manuf 2019;30. https://doi.org/10.1016/j.addma.2019.100810.

[10] Barnett PR, Ghossein HK. A review of recent developments in composites made of recycled carbon fiber textiles. Textiles 2021;1:433–65. https://doi.org/10.3390/textiles1030023.

[11] Hsissou R, Seghiri R, Benzekri Z, Hilali M, Rafik M, Elharfi A. Polymer composite materials: a comprehensive review. Compos Struct 2021;262:113640. https://doi.org/10.1016/j.compstruct.2021.113640.

[12] Zhang J, Chevali VS, Wang H, Wang C-H. Current status of carbon fibre and carbon fibre composites recycling. Compos B Eng 2020;193:108053. https://doi.org/10.1016/j.compositesb.2020.108053.

[13] Post BK, Lind RF, Lloyd PD, Kunc V, Linhal JM, Love LJ. The economics of big area additive manufacturing. University of Texas at Austin; 2016.

[14] Duty C, Ajinjeru C, Kishore V, Compton B, Hmeidat N, Chen X, et al. What makes a material printable? A viscoelastic model for extrusion-based 3D printing of polymers. J Manuf Process 2018;35:526–37. https://doi.org/10.1016/j.jmapro.2018.08.008.

[15] Hill C, Bedsole R, Rowe K, Duty C, Ajinjeru C, Kunc V, et al. Big area additive manufacturing (BAAM) materials development and reinforcement with advanced composites. Knoxville, TN (United States): Inst. for Advanced Composites Manufacturing Innovation (IACMI); 2018. https://doi.org/10.2172/1434289.

[16] Duty CE, Kunc V, Compton B, Post B, Erdman D, Smith R, et al. Structure and mechanical behavior of big area additive manufacturing (BAAM) materials. Rapid Prototyp J 2017;23:181–9. https://doi.org/10.1108/RPJ-12-2015-0183.

[17] Korey M, Rencheck ML, Tekinalp H, Wasti S, Wang P, Bhagia S, et al. Recycling polymer composite granulate/regrind using big area additive manufacturing. Compos B Eng 2023;256:110652. https://doi.org/10.1016/j.compositesb.2023.110652.

[18] Gaikwad V, Ghose A, Cholake S, Rawal A, Iwato M, Sahajwalla V. Transformation of E-waste plastics into sustainable filaments for 3D printing. ACS Sustainable Chem Eng 2018;6:14432–40. https://doi.org/10.1021/acssuschemeng.8b03105.

[19] Brennan LB, Isaac DH, Arnold JC. Recycling of acrylonitrile–butadiene–styrene and high-impact polystyrene from waste computer equipment. J Appl Polym Sci 2002;86:572–8. https://doi.org/10.1002/app.10833.

[20] Cress AK, Huynh J, Anderson EH, O'neill R, Schneider Y, Keleş Ö. Effect of recycling on the mechanical behavior and structure of additively manufactured acrylonitrile butadiene styrene (ABS). J Clean Prod 2021;279:123689. https://doi.org/10.1016/j.jclepro.2020.123689.

[21] Barnett PR, Young SA, Patel NJ, Penumadu D. Prediction of strength and modulus of discontinuous carbon fiber composites considering stochastic microstructure. Compos Sci Technol 2021;211:108857. https://doi.org/10.1016/j.compscitech.2021.108857.

[22] Colón Quintana JL, Slattery L, Pinkham J, Keaton J, Lopez-Anido RA, Sharp K. Effects of fiber orientation on the coefficient of thermal expansion of fiber-filled polymer systems in large format polymer extrusion-based additive manufacturing. Materials 2022;15:2764. https://doi.org/10.3390/ma15082764.

[23] Bernatas R, Dagreou S, Despax-Ferreres A, Barasinski A. Recycling of fiber reinforced composites with a focus on thermoplastic composites. Cleaner Engineering and Technology 2021;5:100272. https://doi.org/10.1016/j.clet.2021.100272.

[24] Copenhaver K, Smith T, Armstrong K, Kamath D, Rencheck M, Bhagia S, et al. Recyclability of additively manufactured bio-based composites. Compos B Eng 2023;255:110617.

[25] Schweizer K, Bhandari S, Lopez-Anido R, Wang L. Recycling large-scale 3D printed polymer composite precast concrete forms. 2023. https://doi.org/10.5281/zenodo.8133142.

[26] Urban furniture project demonstrates green potential for composite 3D printing and recycled materials. 2024. https://www.compositesworld.com/articles/urban-furniture-project-demonstrates-green-potential-for-composite-3d-printing-and-recycled-materials. [Accessed 11 January 2024].

[27] 'Cradle to cradle' research expands composites' 3D-printing possibilities | ORNL n.d. https://www.ornl.gov/news/cradle-cradle-research-expands-composites-3d-printing-possibilities (accessed January 11, 2024).

[28] Tiganis BE, Burn LS, Davis P, Hill AJ. Thermal degradation of acrylonitrile–butadiene–styrene (ABS) blends. Polym Degrad Stabil 2002;76:425–34. https://doi.org/10.1016/S0141-3910(02)00045-9.

[29] Boldizar A, Möller K. Degradation of ABS during repeated processing and accelerated ageing. Polym Degrad Stabil 2003;81:359–66. https://doi.org/10.1016/S0141-3910(03)00107-1.

[30] Scaffaro R, Botta L, Di Benedetto G. Physical properties of virgin-recycled ABS blends: effect of post-consumer content and of reprocessing cycles. Eur Polym J 2012;48:637–48. https://doi.org/10.1016/j.eurpolymj.2011.12.018.

[31] Control of Polymer Properties by Entanglement: A Review - Kong - 2021 - Macromolecular Materials and Engineering - Wiley Online Library n.d. https://onlinelibrary.wiley.com/doi/full/10.1002/mame.202100536 (accessed October 13, 2023)..

[32] Bai X, Liang P, Zhang M, Gong S, Zhao L. Effects of reprocessing on acrylonitrile–butadiene–styrene and additives. J Polym Environ 2022;30:1803–19. https://doi.org/10.1007/s10924-021-02314-z.

[33] Keshtkar M, Heuzey MC, Carreau PJ. Rheological behavior of fiber-filled model suspensions: effect of fiber flexibility. J Rheol 2009;53:631–50. https://doi.org/10.1122/1.3103546.

[34] Shon K, White JL. A comparative study of fiber breakage in compounding glass fiber-reinforced thermoplastics in a buss kneader, modular Co-rotating and counter-rotating twin screw extruders. Polym Eng Sci 1999;39:1757–68. https://doi.org/10.1002/pen.11570.

[35] Ramani K, Bank D, Kraemer N. Effect of screw design on fiber damage in extrusion compounding and composite properties. Polym Compos 1995;16:258–66. https://doi.org/10.1002/pc.750160310.

[36] Brackett J, Cauthen D, Smith T, Kunc V, Duty C. The influence of processing parameters on the transition zone for blended material 3D printing. Oak Ridge, TN (United States): Oak Ridge National Laboratory (ORNL); 2020.

[37] Schneider CA, Rasband WS, Eliceiri KW. NIH Image to ImageJ: 25 years of image analysis. Nat Methods 2012;9:671–5. https://doi.org/10.1038/nmeth.2089.

[38] Lu JZ, Monlezun CJ, Wu Q, Cao QV. Fitting weibull and lognormal distributions to medium-density fiberboard fiber and wood particle length. Wood Fiber Sci 2007:82–94.

[39] Rhodes A. Correlating large-scale AM print parameters to fiber length and mechanical performance of reinforced polymer composites. 2021.

[40] Bing P, Hui-min X, Tao H, Asundi A. Measurement of coefficient of thermal expansion of films using digital image correlation method. Polym Test 2009;28:75–83. https://doi.org/10.1016/j.polymertesting.2008.11.004.

[41] Lyons JS, Liu J, Sutton MA. High-temperature deformation measurements using digital-image correlation. Exp Mech 1996;36:64–70. https://doi.org/10.1007/BF02328699.

[42] Corum T, O'Connell J, Brackett J, Spencer R, Hassen A, Duty C. Characterizing the thermal-induced distortion of large-scale polymer composite printed structures. 2022. https://doi.org/10.26153/tsw/44338.

[43] Physical. Thermal, and mechanical properties of polymers. In: Biosurfaces. John Wiley & Sons, Ltd; 2014. p. 329–44. https://doi.org/10.1002/9781118950623.app1.

[44] Dobkowski Z. Determination of critical molecular weight for entangled macromolecules using the tensile strength data. Rheol Acta 1995;34:578–85. https://doi.org/10.1007/BF00712317.

[45] A proposal to modify the Kelly-Tyson equation to calculate the interfacial shear strength (IFSS) of composites with low aspect ratio fibers. Compos Sci Technol 2020;186:107920. https://doi.org/10.1016/j.compscitech.2019.107920.

[46] Fu S. Effects of fiber length and fiber orientation distributions on the tensile strength of short-fiber-reinforced polymers. Compos Sci Technol 1996;56:1179–90. https://doi.org/10.1016/S0266-3538(96)00072-3.

[47] Tekinalp HL, Kunc V, Velez-Garcia GM, Duty CE, Love LJ, Naskar AK, et al. Highly oriented carbon fiber–polymer composites via additive manufacturing. Compos Sci Technol 2014;105:144–50. https://doi.org/10.1016/j.compscitech.2014.10.009.

[48] Elahi H, Motevasseli AS, Aghazadeh J. The influence of aspect ratio of reinforcing fibers on mechanical properties of gypsum matrix composite panels. 2007. https://www.semanticscholar.org/paper/THE-INFLUENCE-OF-ASPECT-RATIO-OF-REINFORCING-FIBERS-Elahi-Motevasseli/4101aaeaabfffbc452400b2ac6e1f1dbd331443c. [Accessed 2 September 2021].

[49] Halpin JC, Karoos JL. Strength of discontinuous reinforced composites: I. Fiber reinforced composites. Polym Eng Sci 1978;18:496–504. https://doi.org/10.1002/pen.760180612.

[50] Prediction of strength and modulus of discontinuous carbon fiber composites considering stochastic microstructure. Compos Sci Technol 2021;211:108857. https://doi.org/10.1016/j.compscitech.2021.108857.

[51] Becraft ML, Metzner AB. The rheology, fiber orientation, and processing behavior of fiber-filled fluids. J Rheol 1992;36:143–74. https://doi.org/10.1122/1.550359.

[52] Vaxman A, Narkis M, Siegmann A, Kenig S. Short-fiber-reinforced thermoplastics. Part III: effect of fiber length on rheological properties and fiber orientation. Polym Compos 1989;10:454–62. https://doi.org/10.1002/pc.750100610.

[53] Asoodeh F, Aghvami-Panah M, Salimian S, Naeimirad M, Khoshnevis H, Zadhoush A. The effect of fibers' length distribution and concentration on rheological and mechanical properties of glass fiber–reinforced polypropylene composite. J Ind Textil 2022;51:8452S–71S. https://doi.org/10.1177/15280837211043254.

[54] Wittemann F, Kärger L, Henning F. Influence of fiber breakage on flow behavior in fiber length- and orientation-dependent injection molding simulations. J Non-Newtonian Fluid Mech 2022;310:104950. https://doi.org/10.1016/j.jnnfm.2022.104950.

[55] Kotsilkova R. Dynamic rheological properties of glass fiber suspensions. In: Moldenaers P, Keunings R, editors. Theoretical and applied rheology. Amsterdam: Elsevier; 1992. p. 856–8. https://doi.org/10.1016/B978-0-444-89007-8.50385-3.

[56] Crowson RJ, Folkes MJ. Rheology of short glass fiber-reinforced thermoplastics and its application to injection molding. II. The effect of material parameters. Polym Eng Sci 1980;20:934–40. https://doi.org/10.1002/pen.760201404.

[57] Golhin AP, Tonello R, Frisvad JR, Grammatikos S, Strandlie A. Surface roughness of as-printed polymers: a comprehensive review. Int J Adv Manuf Technol 2023;127:987–1043. https://doi.org/10.1007/s00170-023-11566-z.

[58] Das A, Gilmer EL, Biria S, Bortner MJ. Importance of polymer rheology on material extrusion additive manufacturing: correlating process physics to print properties. ACS Appl Polym Mater 2021;3:1218–49. https://doi.org/10.1021/acsapm.0c01228.

[59] Wang T-M, Xi J-T, Jin Y. A model research for prototype warp deformation in the FDM process. Int J Adv Manuf Technol 2007;33:1087–96. https://doi.org/10.1007/s00170-006-0556-9.
[60] Gao X, Qi S, Kuang X, Su Y, Li J, Wang D. Fused filament fabrication of polymer materials: a review of interlayer bond. Addit Manuf 2021;37:101658. https://doi.org/10.1016/j.addma.2020.101658.
[61] Ristic M, Milosevic SDj. Frenkel's theory of sintering. Sci Sinter 2006;38:7–11. https://doi.org/10.2298/SOS0601007R.
[62] Pokluda O, Bellehumeur CT, Vlachopoulos J. Modification of Frenkel's model for sintering. AIChE J 1997;43:3253–6. https://doi.org/10.1002/aic.690431213.
[63] Wool RP, O'Connor KM. A theory crack healing in polymers. J Appl Phys 1981;52:5953–63. https://doi.org/10.1063/1.328526.
[64] Allum J, Moetazedian A, Gleadall A, Silberschmidt VV. Discussion on the microscale geometry as the dominant factor for strength anisotropy in material extrusion additive manufacturing. Addit Manuf 2021;48:102390. https://doi.org/10.1016/j.addma.2021.102390.